

# Medium Effects on $^{51}\text{V}$ NMR Chemical Shifts: A Density Functional Study

Michael Bühl\*<sup>[a]</sup> and Michele Parrinello<sup>[b,c]</sup>

**Abstract:** Car–Parrinello molecular dynamics simulations were performed for  $[\text{H}_2\text{VO}_4]^-$ ,  $[\text{VO}_2(\text{OH}_2)_4]^+$ , and  $[\text{VO}(\text{O}_2)_2(\text{OH}_2)]^-$  in periodic boxes with 30, 28, and 29 water molecules, respectively, employing the BLYP density functional. On the timescale of the simulations, up to 2 ps, well-structured first solvation spheres are discernible for  $[\text{H}_2\text{VO}_4]^-$  and  $[\text{VO}(\text{O}_2)_2(\text{OH}_2)]^-$  containing, on average, eight and ten water molecules, respectively. One of the four

water molecules directly attached to the metal in  $[\text{VO}_2(\text{OH}_2)_4]^+$  is only loosely bound, and the average coordination number of vanadium in aqueous  $\text{VO}_2^+$  is between five and six.  $^{51}\text{V}$  chemical shifts were evaluated at the B3LYP level for

representative snapshots along the trajectories, including the water molecules of the solvent by means of point charges. The resulting averaged  $\delta(^{51}\text{V})$  values are proposed to model the combined effects of temperature (dynamic averaging) and solvent (charge polarization). Both effects are shown to be rather small, of the order of a few dozen ppm. The observed shielding of  $^{51}\text{V}$  in the bis(peroxo) complex with respect to the vanadate species is not reproduced computationally.

**Keywords:** density functional calculations • molecular dynamics • NMR spectroscopy • solvent effects • vanadium

## Introduction

Theoretical chemical shifts have found widespread application in computational chemistry.<sup>[1]</sup> With an appropriate quantum chemical method, the accuracy of the computed  $\delta$  values, compared with experiments, is typically a few percent of the total chemical-shift range of the nucleus under scrutiny. It is frequently observed that the computed chemical shifts are sensitive to structural details. In this case, comparison of theoretical and experimental chemical shifts can afford a structural tool, which has, in favorable cases, been attested a credibility rivaling that of X-ray crystallography.<sup>[2]</sup> The usual procedure involves geometry optimization of the isolated molecule at an appropriate theoretical level, computation of the magnetic shieldings for the static molecule in its equilibrium geometry, and comparison with the NMR experiments conducted in solution at a certain temperature.<sup>[3]</sup> In this procedure it is implicitly assumed that zero-point, temperature, and solvent effects on the chemical shifts are small (or

rather, are very similar for the substrates and the experimental standard, for which a computation has to be performed as well).

Rovibrational effects on shielding tensors  $\sigma$  can be calculated exactly when the potential-energy surface and the shielding tensor surface (i.e. the dependence of  $\sigma$  on the atomic coordinates) are known. In conjunction with a highly sophisticated theoretical model such as GIAO-CCSD(T) (i.e. coupled cluster including single, double, and perturbatively connected triple excitations in a gauge-including atomic orbital scheme),<sup>[4]</sup> remarkably accurate shielding values as a function of temperature can be obtained; these values rival, and sometimes exceed, the precision of corresponding experimental results.<sup>[5]</sup> However, the rigorous calculation of these rovibrational effects, which involves solving the Schrödinger equation for the nuclear motion, is only feasible for very small molecules.<sup>[6]</sup>

Solvent effects on chemical shifts, specifically gas-to-liquid shifts, are known for a number of species, namely those for which accurate gas-phase NMR data extrapolated to zero pressure are available.<sup>[7]</sup> Typical effects are rather small, and they range from a few ppm for  $\delta(^{13}\text{C})$  of organic compounds to approximately  $\Delta\delta(^{18}\text{O}) = 30$  for water,<sup>[8]</sup> but they can also be quite sizeable, for instance, up to approximately  $\Delta\delta(^{77}\text{Se}) = 120$  for  $\text{H}_2\text{Se}$ .<sup>[9]</sup> Not surprisingly, the magnitude of the effect tends to increase with the chemical-shift range of the nucleus.

Exceptionally large shift ranges (in some instances exceeding  $\Delta\delta = 10000$ ) are not uncommon for transition metal nuclei.<sup>[10]</sup> Despite constant progress in the determination of NMR spectra for these formerly exotic nuclei, no experimental gas-phase data are known for transition metal compounds. Trends in the metal shifts in solution have been qualitatively

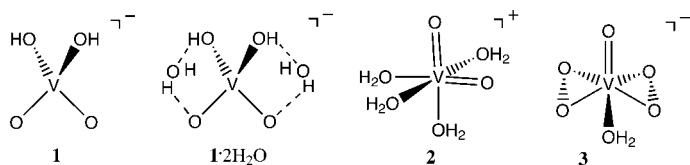
[a] Dr. M. Bühl  
Max-Planck-Institut für Kohlenforschung  
Kaiser-Wilhelm-Platz 1  
45470 Mülheim an der Ruhr (Germany)  
Fax: (+49) 208-306-2996  
E-mail: buehl@mpi-muelheim.mpg.de

[b] Prof. Dr. M. Parrinello  
Max-Planck-Institut für Festkörperforschung  
Heisenbergstrasse 1, 70569 Stuttgart (Germany)

[c] Present address: CSCS Centro Svizzero di Calcolo Scientifico  
Via Cantonale, Galleria 2, 6928 Manno (Switzerland) and  
Physical Chemistry, ETH Hönggerberg HCI  
8093 Zürich (Switzerland)

reproduced computationally for static, isolated molecules by using appropriate density functionals, in particular, the hybrid type such as the popular B3LYP combination.<sup>[11]</sup> In order to assess potential error margins for the computed  $\delta$  values that could arise if one neglects thermal and solvation effects, a simple protocol to estimate such effects is desirable.

For  $\delta(^{51}\text{V})$  of  $[\text{H}_2\text{VO}_4]^-$  (**1**), a typical vanadate species in aqueous solution, a deshielding of  $\Delta\delta = 64$  has been computed upon microsolvation with two water molecules ( $1 \cdot 2\text{H}_2\text{O}$ ).<sup>[12]</sup> For a more conclusive estimate of the solvent effect, addi-



tional water molecules would have to be included. Attempts to optimize correspondingly hydrated (or, in general, solvated) cluster geometries, however, are compromised by the large number of possible minima, which would have to be located. A dynamic treatment would seem to be a promising approach to this problem, in particular since such an approach has been used successfully to model the gas-to-liquid shift for  $\delta(^{18}\text{O})$  in water:<sup>[13, 14]</sup> in order to describe the liquid, classical molecular dynamics (MD) simulations have been performed for large water clusters by using an empirical force field,<sup>[15]</sup> and the chemical shifts have then been calculated by using density functional theory (DFT) for representative snapshots along the simulated trajectory and have been averaged over the time of the simulation.<sup>[13]</sup> Similar results have been obtained in a recent study that employed snapshots from periodic, density functional based MD simulations.<sup>[14, 16]</sup>

**Abstract in German:** *Car–Parrinello-moleküldynamische Simulationen wurden für  $[\text{H}_2\text{VO}_4]^-$ ,  $[\text{VO}_2(\text{OH}_2)_4]^+$  und  $[\text{VO}(\text{O}_2)_2(\text{OH}_2)]^-$  durchgeführt, und zwar in periodischen Boxen mit jeweils 30, 28 und 29 Wassermolekülen, und unter Verwendung des BLYP-Dichtefunktionals. Auf der Zeitskala der Simulationen, bis 2 ps, lassen sich gut strukturierte erste Solvathüllen für  $[\text{H}_2\text{VO}_4]^-$  und  $[\text{VO}(\text{O}_2)_2(\text{OH}_2)]^-$  ausmachen, die im Durchschnitt 8 bzw. 10 Wassermoleküle enthalten. Eines der vier Wassermoleküle, die in  $[\text{VO}_2(\text{OH}_2)_4]^+$  direkt an das Metall koordiniert sind, ist nur schwach gebunden; die mittlere Koordinationszahl des Vanadiums in wässrigem  $\text{VO}_2^+$  liegt hierbei zwischen fünf und sechs.  $^{51}\text{V}$  chemische Verschiebungen wurden für repräsentative Schnappschüsse entlang der Trajektorie auf dem B3LYP-Niveau ermittelt, wobei die Wassermoleküle des Solvens in Form von Punktladungen berücksichtigt wurden. Die so erhaltenen, gemittelten  $\delta(^{51}\text{V})$ -Werte sollen die kombinierten Effekte von Temperatur (thermische Mittelung) und Lösungsmittel (Polarisation) modellieren. Beide Effekte erweisen sich als vergleichsweise klein und liegen in der Größenordnung einiger Dutzend ppm. Die beobachtete Abschirmung des  $^{51}\text{V}$ -Kerns in dem Bis(peroxo)-Komplex relativ zu den Vanadat-Spezies wird in den Rechnungen nicht wiedergegeben.*

For transition metal based compounds such as **1**, the description of the potential-energy surface by a quantum chemical method is mandatory. The DFT-based Car–Parrinello molecular dynamics (CPMD) method is a well-established, cost-efficient MD method that combines approximate DFT-based energy evaluation with classical dynamic propagation.<sup>[17]</sup> In keeping with the widespread applicability of DFT in computational transition metal chemistry,<sup>[18]</sup> the excellent performance of CPMD in this field has been amply demonstrated,<sup>[19]</sup> as has its ability to simulate liquids and solutions.<sup>[20]</sup>

We now present a CPMD study of **1** in aqueous solution as modeled by using a periodic box with a limited number of water molecules. Chemical shifts are evaluated for representative snapshots along the respective trajectories. The same approach is applied to  $[\text{VO}_2(\text{OH}_2)_4]^+$  (**2**), the usual formulation of aqueous vanadate at low pH, and to  $[\text{VO}(\text{O}_2)_2(\text{OH}_2)]^-$  (**3**), the proposed structure of a typical aqueous peroxovanadate (see structures **1–3**). Interest in peroxovanadate complexes has recently been renewed since some of them have been shown to be active as insulin mimetics.<sup>[21]</sup> The simulations reveal interesting details of the coordination sphere around vanadium and the solvent shell around each complex, but predict only relatively small effects on the vanadium chemical shifts.

**Computational details:** Molecular dynamics simulations were performed by using the density functional based Car–Parrinello scheme<sup>[17]</sup> as implemented in the CPMD program.<sup>[22]</sup> Gradient-corrected exchange and correlation functionals according to Becke<sup>[23]</sup> and Lee, Yang, and Parr<sup>[24]</sup> (denoted BLYP) were employed, together with norm-conserving pseudopotentials generated according to the Troullier and Martins' procedure<sup>[25]</sup> and transformed into the Kleinman–Bylander form.<sup>[26]</sup> Periodic boundary conditions were imposed by using cubic supercells with box sizes of 9.5 and 9.8692 Å for the free ions and the ions in aqueous solutions, respectively. Initial geometries for the latter were generated by substituting an appropriate number of water molecules in a snapshot from a well-equilibrated CPMD simulation of liquid water (32 water molecules in a box of the same size)<sup>[27]</sup> with the vanadium complex. Kohn–Sham orbitals were expanded in plane waves up to a kinetic energy cutoff of 80 Ry. In the dynamic simulations a fictitious electronic mass of 600 a.u. and a time step of 0.121 fs were used. To increase the simulation time step, hydrogen was substituted by deuterium. After an equilibration time of 0.5 ps at 300 K, statistical averages and snapshots for the NMR calculations were collected from microcanonical runs 1 ps long. Statistical averages of the aqueous systems were obtained from 2 ps simulations.

Equilibrium geometries for pristine complexes were obtained by optimizing the forces on all atoms with the CPMD program by using the setup detailed above (denoted CP-opt). In addition, geometries were optimized without periodic boundary conditions and the Gaussian-type orbital basis set I, that is, an all-electron Wachters' basis, augmented with two diffuse d and one diffuse p sets for vanadium,<sup>[28]</sup> and 6-31G\* basis<sup>[29]</sup> for all other atoms. The BLYP density functional combination and that according to Becke<sup>[23]</sup> and Perdew<sup>[30]</sup>

(denoted BP86) were employed, as implemented in the Gaussian 98 program package.<sup>[31]</sup>

Magnetic shieldings were computed for equilibrium geometries and for snapshots taken from the MD simulations in the GIAO<sup>[32]</sup> (gauge-including atomic orbitals)-B3LYP method,<sup>[33]</sup> which employed a medium-sized grid and basis I+, that is, basis I augmented with one set of diffuse s and p functions on the ligands. At that level, in conjunction with BP86/I optimized geometries,  $^{51}\text{V}$  chemical shifts have been reproduced to within approximately  $\Delta\delta = 100$  of their experimental values.<sup>[34]</sup> No periodic boundary conditions were imposed in the chemical-shift calculations, and solvent water molecules were not included specifically, but in the form of point charges with values of  $-0.9313$  and  $+0.4656$  for O and H atoms, respectively, as obtained for a single water molecule from natural population analysis at the B3LYP/6-31G\* level. Test calculations for  $1 \cdot 2\text{H}_2\text{O}$  have afforded virtually the same magnetic shielding for vanadium when the two water molecules are included either explicitly or as point charges. Representative snapshots were taken every 20 fs, and water molecules from the six adjacent boxes were also included as point charges. Chemical shifts are reported relative to  $\text{VOCl}_3$ , optimized, or simulated at the same respective level ( $\sigma$  values at  $-2319$ ,  $-2428$ , and  $-2346$  employed BP86/I, BLYP/I, or BLYP/CP-opt geometries, and  $-2386$  for a CPMD simulation averaged over 1 ps, see Figure 1).

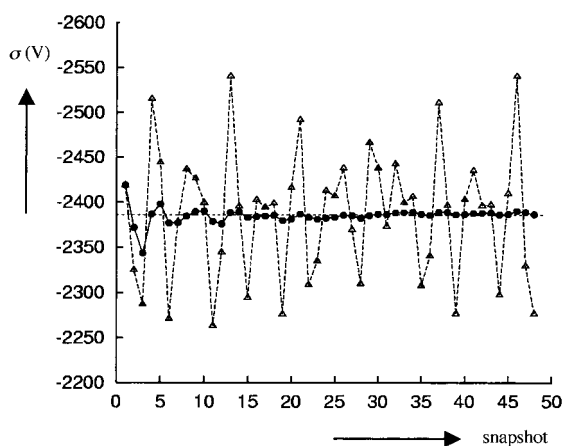


Figure 1. Absolute  $^{51}\text{V}$  magnetic shieldings  $\sigma$  [ppm] for several  $\text{VOCl}_3$  snapshots taken during a 1 ps simulation. Open triangles: raw data; filled circles: running average (average value up to this point).

## Results and Discussion

**$\text{VOCl}_3$ :** Neat  $\text{VOCl}_3$  is the accepted standard in  $^{51}\text{V}$  NMR spectroscopy.<sup>[35]</sup> We have not performed a simulation for this liquid, since this is not essential for the more qualitative purposes of this study. Besides, the inclusion of a sufficiently large number of  $\text{VOCl}_3$  molecules over a long simulation time would be a formidable task in itself. CPMD simulations were performed instead for gaseous  $\text{VOCl}_3$ , and the resulting averaged  $\sigma$  value was also used as a reference value for the solution studies. It should be kept in mind that this procedure could introduce a systematic error for the computed gas-to-

liquid shifts, and that more attention should be paid to the trends in the  $\delta$  values between **1**, **2**, and **3**, rather than to their actual values.

Geometrical data for  $\text{VOCl}_3$  are summarized in Table 1. The equilibrium parameters (columns three to five) are very similar for the various DFT approaches and agree well with the experimental values deduced by gas-phase electron

Table 1. Experimental (GED)<sup>[a]</sup> and computed (DFT) geometrical parameters<sup>[b]</sup> of  $\text{VOCl}_3$ .

Level Parameter	GED	BP86/I <sup>[c]</sup>	BLYP/I	CP-opt <sup>[d]</sup>	CPMD <sup>[e]</sup>
V=O	1.570(5)	1.579	1.589	1.586	1.587(12)
V–Cl	2.142(2)	2.159	2.178	2.159	2.166(38)
O–V–Cl	107.6(1)	108.3	108.4	108.4	108.3(44)

[a] Gas-phase electron diffraction, from ref. [36]. [b] Distances in Å, angles in degrees (in parentheses: standard deviation). [c] All-electron orbital basis, from ref. [34]. [d] Pseudopotentials and plane-wave basis, minimized with the CPMD program. [e] Average values from a 1 ps simulation at approximately 300 K.

diffraction<sup>[36]</sup> (GED). The mean bond lengths averaged over a 1 ps CPMD run confirm the expected slight increase with respect to their equilibrium values (compare the last two columns in Table 1).

Despite the small *average* bond-length elongation, large *individual* variations occur during the simulations at 300 K, as reflected in the standard deviations included in Table 1.<sup>[37]</sup> For instance, maximum and minimum V–Cl distances of 2.260 and 2.074 Å, respectively, are encountered. In view of the large bond-length/shielding derivatives deduced or computed for transition metal nuclei,<sup>[38]</sup> large effects on the computed  $\sigma$  values are to be expected. Indeed, fluctuations over several hundred ppm are obtained for the snapshots from the simulation (open triangles in Figure 1). However, the running average, that is the average over all values up to a given point, is remarkably constant after approximately 15 snapshots. The same is found for nearly all the other simulations of this study, and this result suggests that the simulation time is sufficient.

The averaged  $\sigma$  value is deshielded by 40 ppm with respect to the equilibrium value.<sup>[39]</sup> This is a small number compared with the  $^{51}\text{V}$  chemical-shift range (which exceeds 4000 ppm),<sup>[35]</sup> and this number reflects the moderate temperature effects on the (average) bond lengths. Two questions have to be addressed now: firstly, are the temperature effects on the magnetic shieldings of other vanadium compounds of the same order of magnitude, and secondly, how large is, in relation to the temperature effects, that of the solvent?

**$[\text{H}_2\text{VO}_4]^-$ :** Speciation of vanadate(v) in aqueous solution involves complex equilibria between various mono- and oligonuclear clusters, and the composition critically depends on concentration and pH.<sup>[40]</sup> In dilute solutions at pH 7, the dominant species is  $[\text{H}_2\text{VO}_4]^-$  (**1**).  $\delta(^{51}\text{V})$  values of isolated **1** are computed, depending on the computational model, in the

Table 2. Experimental and computed (GIAO-B3LYP)  $^{51}\text{V}$  chemical shifts.

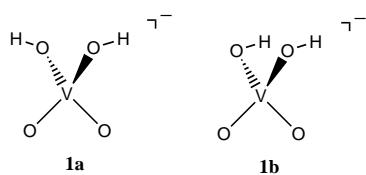
Level of approximation <sup>[a]</sup>	$[\text{H}_2\text{VO}_4]^-$	$\text{VO}_2^+ \cdot 4\text{H}_2\text{O}$		$[\text{VO}(\text{O}_2)_2(\text{OH}_2)]^-$
	<b>1</b>	( <b>2a</b> )	<b>2b</b>	<b>3</b>
experiment/ $\text{H}_2\text{O}$	-560		-545	-692
//BP86/I	-629	(-607)	-656	-629
//BLYP/I	-672	(-639)	-688	-636
//CP-opt	-691	(-638)	-664	-623
//CPMD	-717		-662	-564
//CPMD/ $\text{H}_2\text{O}$ <sup>[b]</sup>	-712		-694	-655

[a] See footnotes [c]–[e] in Table 1. [b] Average values from a 1 ps simulation at approximately 300 K in a periodic water box.

range between  $\delta = -629$  and  $-691$  (see entries two to four in Table 2). During the 1 ps simulation for the pristine anion, conformational changes occurred in the VOH moieties: starting from the equilibrated configuration corresponding to **1a** (idealized  $C_2$  symmetry), both OH groups first rotated simultaneously about their respective VO axes to afford the enantiomer of **1a**. Subsequently, one of the OH groups rotated back to its original position, which resulted in a configuration corresponding to **1b** (idealized  $C_s$  symmetry). Apparently, these isomers are very similar in energy and are separated by very low barriers. Little difference in the  $^{51}\text{V}$  chemical shifts is to be expected between **1a** and **1b** (in fact, a mere  $\Delta\delta = 3$  difference is computed at the B3LYP/I + //BP86/I level). Hence, the time-averaged magnetic shielding will be governed by the vibrational motion. A deshielding of 14 ppm is obtained in going from the equilibrium to the averaged  $\sigma$  value. This temperature effect is smaller than that for  $\text{VOCl}_3$  discussed above, but is certainly of the same order of magnitude. Since the computed deshielding is larger for the  $\sigma$  value of  $\text{VOCl}_3$  than for that of **1**, the predicted effect on  $\delta(^{51}\text{V})$  of the latter is a net upfield shift (shielding),  $\Delta\delta = -26$  (compare entries CP-opt,  $\delta = -691$ , and CPMD,  $\delta = -717$  in Table 2).

During the simulation of **1** in a periodic box with 30 water molecules, one interconversion from **1a** to **1b** and back was observed in the initial 0.5 ps equilibration run, but not in the subsequent 2 ps simulation. The conformational fluxionality of **1** appears thus to be attenuated by the solvent. Before discussing the chemical shifts, we will turn to the structure of the solvation shell around **1**.

The two OH moieties in **1** can act as hydrogen-bond donors to solvent molecules, and all four oxygen atoms can accept such H-bonds from the surrounding water. In typical hydrogen-bonded systems containing  $\text{O}-\text{H}\cdots\text{O}$  moieties, the  $\text{O}\cdots\text{O}$  distance is smaller than 3.5 Å, and the OH-bond is directed towards the second oxygen atom such that the  $\text{O}-\text{H}\cdots\text{O}$  angle is larger than 140 degrees.<sup>[41]</sup> Based on these purely geometrical criteria, during the 2 ps simulation the average number of water molecules coordinated to **1** is around eight



(around seven with  $\text{O}\cdots\text{O}$  distances smaller than 3.0 Å). A typical configuration is depicted in Figure 2, which illustrates

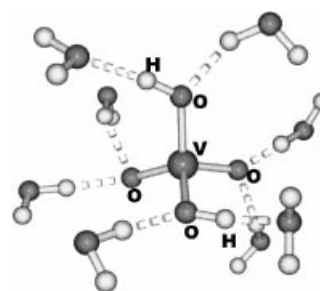


Figure 2. Representative snapshot of **1** in water that shows eight H-bonded solvent molecules.

how the two terminal oxygen atoms accept two H-bonds each, while the two OH moieties are both H-bond donors and acceptors.

This first solvation shell around **1** is not fixed during the simulation. Water molecules can be exchanged reversibly between this shell and the remaining solvent, and at least five such processes can be detected during the 2 ps simulation (three in the first ps, in which the snapshots for the NMR calculations were taken). In Figure 3 such an exchange

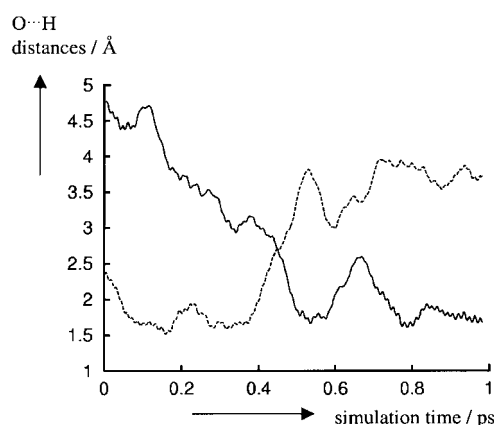


Figure 3. Exchange of a water molecule between the first solvation sphere around **1** and solution as monitored by the  $\text{O}\cdots\text{H}$  distances between a vanadate oxygen atom and the protons of the leaving and incoming water molecules.

process is illustrated by monitoring two  $\text{O}\cdots\text{HO}$  distances from simultaneously forming and breaking hydrogen bonds. A certain near-range order is also apparent from the computed VO pair correlation function<sup>[42]</sup> (Figure 4a). Apart from the two spikes below 2 Å corresponding to the two types of VO-bonds, a shallow maximum is indicated between 3.5 and 4.5 Å, part of which is attributable to the first solvation sphere. That this maximum corresponds to approximately ten oxygen atoms, rather than eight, must be due to the presence of additional water molecules within this radius which are, apparently, not H-bonded to the vanadate. In order to address the question of a possible second solvation sphere, longer

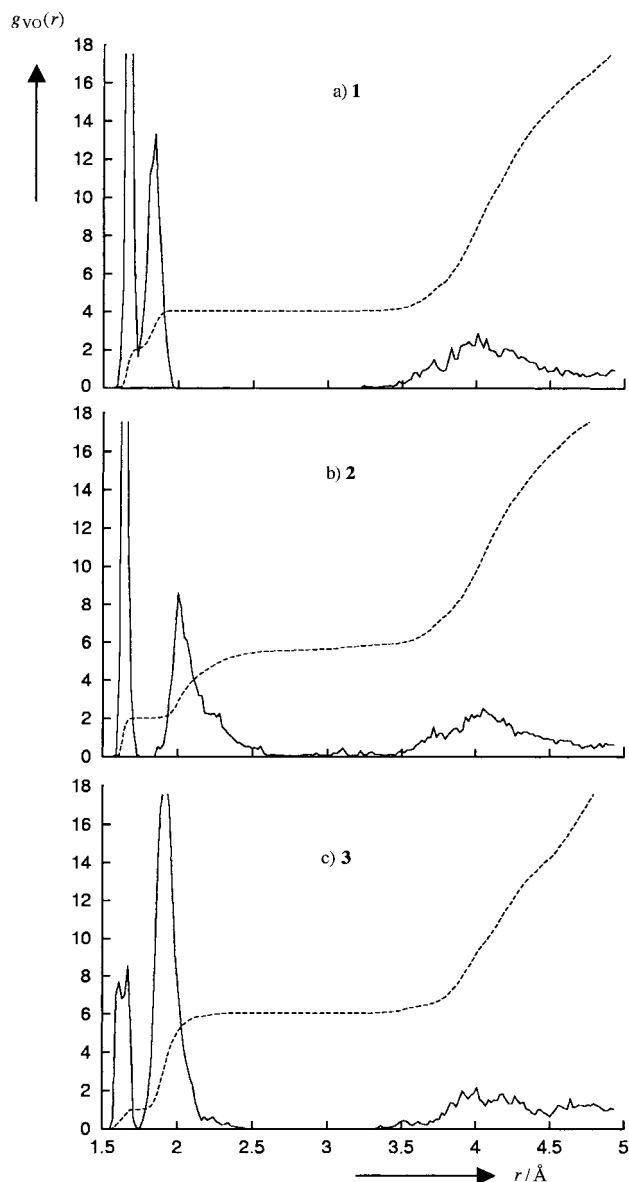


Figure 4. Solid line: simulated vanadium–oxygen pair correlation functions  $g(r)$  in aqueous solution of **1**, **2**, and **3** (top to bottom); dashed:  $n_{\text{O}}(r) = \rho_{\text{O}} \int g(r) 4\pi r^2 dr$ , which integrates to the total number of oxygen atoms in a sphere with radius  $r$  around vanadium.

simulation times and, in particular, larger boxes would be required. For the purposes of this study, it is important to note that with the chosen setup, a hydration shell around **1** is discernible which is in equilibrium with the surrounding solvent. The introduction of artifacts due to an arbitrarily chosen starting point is thus unlikely, and snapshots along the simulated trajectory should be realistic models for an aqueous solution.

What is the computed medium effect on the  $^{51}\text{V}$  chemical shift of **1**? Interestingly, the  $\sigma$  values averaged along a 1 ps trajectory are almost the same for pristine **1** and for **1** in water, which affords a predicted gas-to-liquid shift of only  $\Delta\delta = +5$  (compare CPMD and CPMD/ $\text{H}_2\text{O}$  entries in Table 2). A much larger effect,  $\Delta\delta = +64$ , had been computed on going from **1** to the microsolvated complex  $\mathbf{1} \cdot 2\text{H}_2\text{O}$  (structures **1–3**). Apparently, this large value is an artifact of the tightly

bound cluster structure with its multiply H-bonded water molecules. No such configurations are encountered in the actual solvation shell around aqueous **1** (see Figure 2).<sup>[43]</sup>

The combined effect on  $\delta(^{51}\text{V})$  of a larger number of more weakly attached water molecules in aqueous **1** is thus smaller than that of the two, more tightly attached ones in  $\mathbf{1} \cdot 2\text{H}_2\text{O}$ . When computations were performed for the same snapshots with and without the point charges representing the solvent, the final averaged shielding values were the same within 1 ppm. The effect of solvation on  $\delta(^{51}\text{V})$  is thus indirect: it is the change of geometrical parameters (or their variation over time) brought about by the solvent that is primarily responsible for the chemical shifts. The same has been surmised in other cases, for instance for  $\delta(^{11}\text{B})$  in aqueous  $\text{BH}_3\text{--NH}_3$ .<sup>[44]</sup> To be on the safe side, however, point charges were included in the subsequent chemical-shift evaluations in water.

In conclusion, the temperature effect on  $\delta(^{51}\text{V})$  of **1** is computed to be more important than that of the solvent, but both are small anyway. In order to see if this result is transferable to other vanadium compounds, we will now discuss two other typical oxovanadium(v) species.

**$\text{VO}_2^+$  (aq):** Lowering the pH of dilute aqueous solutions of vanadate **1** results in double protonation of the latter, and the predominant product is usually formulated as  $\text{VO}_2^+$ , which is believed to be six-coordinated with a *cis*- $\text{VO}_2^+$  moiety and four complexed  $\text{H}_2\text{O}$  molecules. Thermodynamic data for the appropriate protonation equilibria have been taken as evidence for a corresponding expansion of the coordination number about vanadium<sup>[45]</sup> (that is, from four in **1** to six). Indeed, a minimum can be located for  $[\text{VO}_2(\text{OH}_2)_4]^+$  with a distorted octahedral coordination sphere around the metal (**2a**, Figure 5). When the BP86 geometries are employed, quite similar  $\delta(^{51}\text{V})$  values (within  $\Delta\delta = 22$ ) are computed for pristine **1a** and **2a**, in apparent accord with experiments (Table 2). Use of BLYP geometries results in somewhat more disparate values (up to  $\delta = 53$  difference for the CP-opt structures).

However, pristine **2a** turned out to be unstable in a molecular dynamic simulation: very rapidly, within the first 0.5 ps equilibration period, one water molecule is expelled from the coordination sphere of the metal and remains only

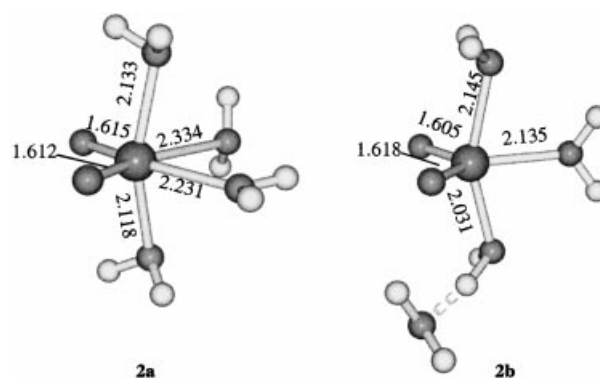


Figure 5. Six-coordinated (**2a**, left) and five-coordinated (**2b**, right) hydrated  $\text{VO}_2^+$  complexes, including BP86/I optimized bond lengths [Å].

H-bonded to one of the other water ligands. The resulting pentacoordinate species  $\text{VO}_2(\text{OH}_2)_3^+ \cdot \text{H}_2\text{O}$  (**2b**) is also a minimum on the potential-energy surface (see Figure 5) and is indeed lower in energy than **2a** on all levels considered (namely by 4.8, 4.4, and 3.9 kcal mol<sup>-1</sup> at the BP86/I, BLYP/I, and B3LYP/I + //BLYP/I level, respectively). Given the facile rearrangement from **2a** to **2b** during the unconstrained MD run, which is indicative of a very low barrier between both, isolated **2a** should not exist in the gas phase.

The situation in bulk solution could be different, however: if the fourth water ligand at the vanadium were stabilized by an inter- rather than an intramolecular hydrogen bond, hexacoordination could prevail. Indeed, during the 0.5 ps equilibration time, all four water molecules appeared to remain coordinated to vanadium, and they performed several V–O stretching motions. After an additional 0.2 ps, one H<sub>2</sub>O molecule moved away from the complex, up to a V...O distance above 3 Å, that is, well beyond direct bonding, and returned to the metal immediately. After another 0.4 ps, the same ligand moved even farther away, up to 4 Å, and returned approximately 1 ps later. The evolution of the corresponding VO separation is shown in Figure 6 (together with that for pristine **2a**).

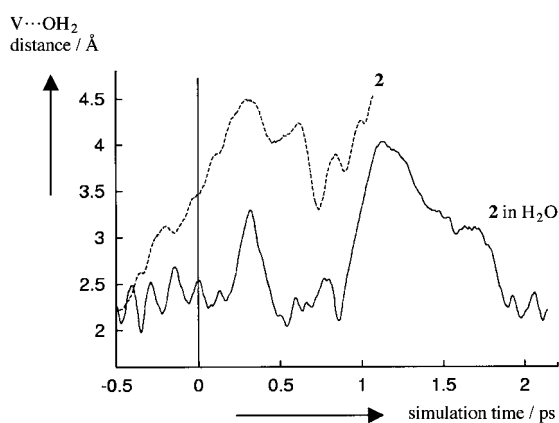


Figure 6. Variation of the distance between vanadium and the labile water ligand in **2** over a 2 ps simulation time, including the preceding 0.5 ps equilibration (dashed: pristine **2**; solid: **2** in water box).

Not considering the first 0.5 ps of equilibration, we found that the 2 ps simulation of **2** in water finds vanadium six-coordinated for roughly half of the time, and five-coordinated for the remainder. For a quantitative estimate of the average coordination number many more reversible dissociation and association processes would have to be sampled, in other words much longer simulation times would be necessary. In any event, the average coordination number will be neither exactly five nor six, but will assume an intermediate value. From the VO pair correlation function in Figure 4b integrated up to VO distances of 2.6 Å, a value of 5.5 is obtained for this average coordination number.

What are the effects of thermal motion and solvent on the <sup>51</sup>V chemical shifts of **2**? As a result of the instability of free **2a**, the CPMD simulation without solvent actually probes the temperature effect for pure **2b**. Virtually the same thermal effect on the <sup>51</sup>V magnetic shielding is obtained for **2b** as for

$\text{VOCl}_3$ , and this has essentially no effect on the computed  $\delta$  value (compare CP-opt and CPMD entries in Table 2). In order to estimate the solvent effect on  $\delta(^{51}\text{V})$  of aqueous **2**, a snapshot sampling over a larger simulation time was necessary, as it took somewhat more than 1 ps for the running average of  $\sigma$  to converge. The final result reveals a more pronounced solvation effect on  $\delta(^{51}\text{V})$ ,  $\delta = 32$  (compare CPMD and CPMD/H<sub>2</sub>O entries). Incidentally, the observed shift difference between **1** and **2**,  $\Delta\delta = +15$ , is well reproduced, both in sign and in magnitude, by the CPMD/H<sub>2</sub>O values,  $\Delta\delta = +18$ .

Interestingly, in the early stage of the simulation (approximately 0.3 ps after the equilibration), a proton transfer occurred from a H<sub>2</sub>O ligand (*cis* to a V=O unit) to a water molecule from the surrounding solvent to afford neutral  $[\text{VO}(\text{OH})(\text{OH}_2)_3]$ , H-bonded to H<sub>3</sub>O<sup>+</sup>. This complex was stable for less than 0.3 ps after which it reverted back to **2a**. Only limited conclusions can be drawn from this single event, but its occurrence is quite consistent with the observation that cationic, hydrated VO<sub>2</sub><sup>+</sup> is only stable at high H<sub>3</sub>O<sup>+</sup> concentrations and undergoes deprotonation when the pH is raised to 7, eventually affording anionic species.<sup>[46]</sup> It is reasonable to assume that the actual deprotonation of **2** happens on a longer timescale than the 2 ps studied here, so that this simulation in neutral solution should be a good model for the real system under acidic conditions.

In summary, the solution structure of **2** is more complicated than that of **1**, since for the former a variable coordination number of vanadium is revealed. There are indications that the combined thermal and solvent effects on  $\delta(^{51}\text{V})$  of **1** and **2** are small,  $\Delta\delta = 21$  and 32, respectively (compare CP-opt and CPMD/H<sub>2</sub>O results in Table 2). Whereas for **1** thermal effects are more important (see difference between CP-opt and CPMD entries), the solvent effect is more predominant in the case of **2** (see CPMD vs. CPMD/H<sub>2</sub>O entries). At all levels, the computed <sup>51</sup>V chemical shifts of **1** and **2** are too negative when compared with those from experiments, and absolute errors can exceed  $\Delta\delta = 150$ . As mentioned above, these apparent deviations may at least in part be due to shortcomings in the description of the standard. Nevertheless, the close similarity (and for the CP-derived results also the sequence) of both  $\delta$  values is satisfactorily reproduced in the computations.

**[VO(O<sub>2</sub>)<sub>2</sub>(OH<sub>2</sub>)<sup>-</sup>]**: How well are the theoretical approaches suited to reproduce trends involving larger shift differences? The <sup>51</sup>V nuclei in diperoxovanadate complexes are in general substantially shielded with respect to those in comparable vanadate complexes. For instance,  $\delta(^{51}\text{V}) = -692$  is obtained for the main reaction product of hydrogen peroxide with **1** or **2** ( $\delta = -560$  and  $-545$ , respectively) above pH 4.<sup>[40, 47]</sup> Under these conditions,  $[\text{VO}(\text{O}_2)_2]^-$  (aq) is the predominant species, and a plausible structure for the species in solution has been put forward based on density functional computations for  $[\text{VO}(\text{O}_2)_2(\text{OH}_2)]^-$  (**3**).<sup>[47]</sup>

The coordination geometry about vanadium in **3** can be described as a pentagonal pyramid with an apical V=O group. Even though there are precedents for such a six-coordinated species involving the VO(O<sub>2</sub>)<sub>2</sub> fragment in the solid state,<sup>[48]</sup>

most complexes with this moiety are seven-coordinated with an additional donor atom *trans* to the oxo ligand.<sup>[49]</sup> Attempts to locate such a pentagonal bipyramidal structure corresponding to **3** with an additional water ligand bound to vanadium were unsuccessful, as this additional water molecule was expelled from the coordination sphere of the metal during optimization (or equilibration in an MD run) and remained only H-bonded to a peroxo ligand.

In contrast to the observed upfield shift of  $\delta(^{51}\text{V})$  in going from **1** to **3**, no such increased shielding is computed for the static optimized structure of **3**, irrespective of the level of geometry optimization. When the BP86/I geometries are employed, the same chemical shifts are computed for **1** and **3**, and the use of BLYP optimized structures results in a deshielding of **3** versus **1**, that is, the opposite of the trend found experimentally (Table 2). An additional large ( $\Delta\delta = 60$ ) upfield shift is found during the 1 ps simulation of pristine **3** (compare CP-opt and CPMD entries in Table 2). This deshielding is probably related to the dynamics of the coordinated water molecule in **3**, which undergoes large-amplitude V–O stretching vibrations. The CP-optimized V–O(H<sub>2</sub>) distance, 2.269 Å, is increased to an average of 2.394 Å at approximately 300 K, with minimum and maximum values of 2.041 and 2.769 Å, respectively.

From this result one might expect the water ligand in **3** to be quite labile and readily exchangeable with solvent molecules in aqueous solution. Quite unexpectedly, the V–O(H<sub>2</sub>) bonding is reinforced during the simulation in water, as the averaged distance is reduced to 2.082 Å (between 1.916 and 2.423 Å) in the water box, and no exchange occurs during the whole 2.5 ps. There is evidence from  $^{51}\text{V}$  NMR studies of **3** and other peroxovanadate complexes that fast exchange occurs between solvent molecules and ligands of vanadium.<sup>[50]</sup> Very likely, this process takes place at timescales longer than those simulated in the present study.

As in the case of **1**, a distinct hydration sphere can be discerned for **3**. During the final picosecond of the simulation, the average number of H-bonds between **3** and the solvent is around ten, according to the geometrical criteria detailed above. The water ligand in **3** donates two strong hydrogen bonds to two solvent molecules, whereas the remaining oxo and peroxo atoms accept one or two H-bonds each from the surrounding solvent. No water molecule from the solvent is approaching the potential coordination site *trans* to the oxo ligand. According to the VO pair correlation function integrated up to VO distances of 2.5 Å (Figure 4c), the average coordination number about vanadium is exactly six.

Consistent with the shortening of the V–O(H<sub>2</sub>) bond in going from pristine to aqueous **3**, a notable solvation effect is computed for  $\delta(^{51}\text{V})$ , namely an upfield shift of  $\Delta\delta = 91$  (compare CPMD and CPMD/H<sub>2</sub>O data<sup>[51]</sup> in Table 2). The combined thermal and solvent effects, that is, the difference between the CP-opt and CPMD/H<sub>2</sub>O-derived  $\delta$  values, are small and are shielding ( $\Delta\delta = -32$ ). Thus, the correct sequence of  $^{51}\text{V}$  resonances of **1** and **3** is not reproduced by the simulations. The reason for this discrepancy between theory and experiment is unclear at this point. Further work is needed to improve the accuracy of the computations. Special

attention should be given to the density functional employed in the CPMD simulation. The BLYP combination, chosen because of its good performance in the description of liquid water,<sup>[27]</sup> is probably not the best choice for transition metal complexes.

## Conclusion

We have devised a computational protocol for the estimation of thermal and solvent effects on vanadium chemical shifts in hydrated oxo and peroxo complexes. To our knowledge, these are the first computations of dynamically averaged chemical shifts for a transition metal nucleus. Not surprisingly, thermal and solvent effects are noticeable when weakly bound ligands are present and/or flat regions of the potential-energy surface are involved. Compared with the approximately  $\Delta\delta = 4000$  chemical-shift range of  $^{51}\text{V}$ , however, the combined changes brought about by thermal averaging and the solvent are quite small, and are of the order of a few dozen ppm. At least for d<sup>0</sup> vanadium complexes with oxygen donors, these results may serve as justification for the use of static equilibrium geometries when comparing computed chemical shifts with solution data at ambient temperature. Further studies should be performed in order to test if the same holds for other transition metal compounds as well.

While the small difference in  $\delta(^{51}\text{V})$  values between the vanadate species **1** and **2** is well reproduced in the dynamic calculations, the observed shielding of the metal in the bis(peroxo) complex **3** is not. Since inclusion of thermal and solvent effects in the computations does not resolve this discrepancy between theory and experiment, closer attention should be paid to the performance of DFT-based methods for  $\delta(^{51}\text{V})$  of peroxovanadium compounds in general.

Possible problems in the NMR computations notwithstanding, the dynamic simulations of the vanadium complexes reveal interesting details of the coordination geometries and the solvent shells in aqueous solution. Well-structured hydration shells are discernible, which are in dynamic equilibrium with the surrounding solvent on the picosecond timescale. When, as in **2** or **3**, weakly coordinated water ligands are bound to vanadium, bonding to the metal is strengthened on going from the pristine complexes to the solution. This change may affect the average coordination number about the metal center, which in **2** is raised from 5 in the gas phase to approximately 5.5 in water. The sensitivity of the equilibrium  $\delta(^{51}\text{V})$  value to the coordination number and, hence, the computed solvent effect, is relatively small in this case. In cases with a more pronounced dependence of the chemical shifts on the coordination sphere, larger medium effects on the metal chemical shifts are to be expected.

## Acknowledgements

M.B. wishes to thank Prof. W. Thiel for his continuing support, the Deutsche Forschungsgemeinschaft for a Heisenberg fellowship, and the Stuttgart group for invaluable assistance with the CPMD program, in particular A. Gambirasi, V. Merigalli, and M. Boero. Computations were performed on IBMRS/6000 workstations at the MPI Stuttgart, and on Compaq XP1000 and ES40 workstations at the MPI Mülheim.

- [1] T. Helgaker, M. Jaszunski, K. Ruud, *Chem. Rev.* **1999**, *99*, 293.
- [2] T. Onak, J. Tseng, M. Diaz, D. Tran, J. Arias, S. Herrera, D. Brown, *Inorg. Chem.* **1993**, *32*, 487.
- [3] M. Bühl in *Encyclopedia of Computational Chemistry* (Eds.: P. v. R. Schleyer, N. L. Allinger, P. A. Kollman, T. Clark, H. F. Schaefer, J. Gasteiger, P. R. Schreiner), Wiley, Chichester, **1998**, p. 1835.
- [4] J. Gauss, J. F. Stanton, *J. Chem. Phys.* **1996**, *104*, 2574.
- [5] D. Sundholm, J. Gauss, A. Schäfer, *J. Chem. Phys.* **1996**, *105*, 11051.
- [6] For a procedure applicable, in principle, to larger systems, see: a) K. Ruud, P.-O. Åstrand, P. R. Taylor, *J. Chem. Phys.* **2000**, *112*, 2668; b) K. Ruud, P.-O. Åstrand, P. R. Taylor, *J. Am. Chem. Soc.* **2001**, *123*, 4826.
- [7] For instance: C. J. Jameson, *Chem. Rev.* **1991**, *91*, 1375.
- [8] a) A. E. Florin, M. Alei, *J. Phys. Chem.* **1967**, *47*, 4268; b) W. T. Raynes, *Mol. Phys.* **1983**, *49*, 443.
- [9] P. D. Ellis, J. D. Odom, A. S. Lipton, Q. Chen, J. M. Gulick in *Nuclear Magnetic Shieldings and Molecular Structure: NATO ASI Series* (Ed.: J. A. Tossell), Kluwer, Amsterdam, **1993**, p. 539.
- [10] *Transition Metal Nuclear Magnetic Resonance* (Ed.: P. S. Pregosin), Elsevier, Amsterdam, **1991**.
- [11] For instance: M. Bühl, M. Kaupp, V. G. Malkin, O. L. Malkina, *J. Comput. Chem.* **1999**, *20*, 91.
- [12] M. Bühl, *J. Comput. Chem.* **1999**, *20*, 1254.
- [13] V. G. Malkin, O. L. Malkina, G. Steinebrunner, H. Huber, *Chem. Eur. J.* **1996**, *2*, 452.
- [14] B. G. Pfommer, F. Mauri, S. G. Louie, *J. Am. Chem. Soc.* **2000**, *122*, 123.
- [15] Empirical MD simulations have also been used in the evaluation of solvent effects on the fluorine shielding in fluorobenzene: E. Y. Lau, J. T. Gerig, *J. Am. Chem. Soc.* **1996**, *118*, 1194.
- [16] Medium effects on chemical shifts can also be modeled for static clusters of increasing size in the quantum cluster equilibrium method, see for instance: R. Ludwig, F. Weinhold, T. C. Farrar, *Mol. Phys.* **1999**, *97*, 479.
- [17] R. Car, M. Parrinello, *Phys. Rev. Lett.* **1985**, *55*, 2471.
- [18] a) W. Koch, M. C. Holthausen, *A Chemist's Guide to Density Functional Theory*, Wiley-VCH, Weinheim, **2000**; b) See also the special issue of *Chem. Rev.* **2000**, *100*, 351 on Computational Transition Metal Chemistry.
- [19] For selected recent applications see for example: a) P. Carloni, M. Sprik, W. Andreoni, *J. Phys. Chem. B* **2000**, *104*, 823; b) C. Rovira, M. Parrinello, *Int. J. Quantum Chem.* **2000**, *80*, 1172; c) J. J. Mortensen, M. Parrinello, *J. Phys. Chem. B* **2000**, *104*, 2901; d) M. Boero, M. Parrinello, S. Huffer, H. Weiss, *J. Am. Chem. Soc.* **2000**, *122*, 501; e) A. Magistrato, J. Van de Vondelle, U. Röthlisberger, *Inorg. Chem.* **2000**, *39*, 5553.
- [20] See for instance: M. Sprik, *J. Phys. Condens. Matter* **2000**, *12*, A161, and references therein.
- [21] See for instance: *Vanadium Compounds, Chemistry, Biochemistry, and Therapeutic Applications* (Eds.: A. S. Tracey, D. C. Crans), ACS Symp. Ser. **1998**, *711*.
- [22] J. Hutter, A. Alavi, T. Deutsch, M. Bernasconi, S. Goedecker, D. Marx, M. Tuckerman, M. Parrinello, CPMD Version 3.3a, Max-Planck-Institut für Festkörperforschung and IBM Research Laboratory (**1995–1999**).
- [23] A. D. Becke, *Phys. Rev. A* **1988**, *38*, 3098.
- [24] C. Lee, W. Yang, R. G. Parr, *Phys. Rev. B* **1988**, *37*, 785.
- [25] N. Troullier, J. L. Martins, *Phys. Rev. B* **1991**, *43*, 1993.
- [26] L. Kleinman, D. M. Bylander, *Phys. Rev. Lett.* **1982**, *48*, 1425.
- [27] M. Sprik, J. Hutter, M. Parrinello, *J. Chem. Phys.* **1996**, *105*, 1142.
- [28] a) A. J. H. Wachters, *J. Chem. Phys.* **1970**, *52*, 1033; b) P. J. Hay, *J. Chem. Phys.* **1977**, *66*, 4377.
- [29] a) W. J. Hehre, R. Ditchfield, J. A. Pople, *J. Chem. Phys.* **1972**, *56*, 2257; b) P. C. Hariharan, J. A. Pople, *Theor. Chim. Acta.* **1973**, *28*, 213.
- [30] a) J. P. Perdew, *Phys. Rev. B* **1986**, *33*, 8822; b) J. P. Perdew, *Phys. Rev. B* **1986**, *34*, 7406.
- [31] Gaussian98 (Revision A.7), M. J. Frisch, G. W. Trucks, H. B. Schlegel, G. E. Scuseria, M. A. Robb, J. R. Cheeseman, V. G. Zakrzewski, J. A. Montgomery, R. E. Stratman, J. C. Burant, S. Dapprich, J. M. Milliam, A. D. Daniels, K. N. Kudin, M. C. Strain, O. Farkas, J. Tomasi, V. Barone, M. Cossi, R. Cammi, B. Mennucci, C. Pomelli, C. Adamo, S. Clifford, J. Ochterski, G. A. Petersson, P. Y. Ayala, Q. Cui, K. Morokuma, D. K. Malick, A. D. Rabuck, K. Raghavachari, J. B. Foresman, J. Cioslowski, J. V. Ortiz, A. G. Baboul, B. B. Stefanov, C. Liu, A. Liashenko, P. Piskorz, I. Komaromi, R. Gomperts, R. L. Martin, D. J. Fox, T. Keith, M. A. Al-Laham, C. Y. Peng, A. Nanayakkara, C. Gonzalez, M. Challacombe, P. M. W. Gill, B. G. Johnson, W. Chen, M. W. Wong, J. L. Andres, C. Gonzales, M. Head-Gordon, E. S. Replogle, J. A. Pople, Gaussian, Inc., Pittsburgh PA, **1998**.
- [32] a) R. Ditchfield, *Mol. Phys.* **1974**, *27*, 789; b) K. Wolinski, J. F. Hinton, P. Pulay, *J. Am. Chem. Soc.* **1990**, *112*, 8251.
- [33] GIAO-DFT implementation: J. R. Cheeseman, G. W. Trucks, T. A. Keith, M. J. Frisch, *J. Chem. Phys.* **1996**, *104*, 5497.
- [34] M. Bühl, F. A. Hamprecht, *J. Comput. Chem.* **1998**, *19*, 113.
- [35] See for instance D. Rehder in *Transition Metal Nuclear Magnetic Resonance* (Ed.: P. S. Pregosin), Elsevier, Amsterdam, **1991**, p. 1.
- [36] a) K. Karakida, K. Kuchitsu, *Inorg. Chim. Acta* **1975**, *13*, 113; b) H. Oberhammer, J. Strähle, *Z. Naturforsch. A* **1975**, *30*, 296.
- [37] The large standard deviations are a consequence of the classical propagation, which samples too many configurations near the potential wells as a result of the low velocities in those regions; in the vibrational ground state, the main contributions arise from configurations near the equilibrium structure.
- [38] See for instance a) C. J. Jameson, D. Rehder, M. Hoch, *J. Am. Chem. Soc.* **1987**, *109*, 2589; b) N. Godbout, E. Oldfield, *J. Am. Chem. Soc.* **1997**, *119*, 8065; c) W. Leitner, M. Bühl, R. Fornika, C. Six, W. Baumann, E. Dinjus, M. Kessler, C. Krüger, A. Ruffinska, *Organometallics* **1999**, *18*, 1196.
- [39] It should be noted that this value only represents the “classical” thermal effect and is not averaged over the zero-point motion. For first-row nuclei, such zero-point effects are larger than that of the temperature, see for instance ref. [5].
- [40] See for instance D. Rehder in *Metal Ions in Biological Systems, Vol. 31* (Eds.: H. Sigel, A. Sigel), Marcel Dekker, New York, **1995**, p. 1.
- [41] For instance: E. Schwegler, G. Galli, F. Gygi, *Phys. Rev. Lett.* **2000**, *84*, 2429.
- [42] For the definition of the pair correlation function see for example: M. P. Allen, D. J. Tildesley, *Computer Simulation of Liquids*, Clarendon, Oxford, **1987**.
- [43] For an 1·2H<sub>2</sub>O cluster such a minimum can also be located with a CP optimization; during a CPMD run at 300 K, however, one of the water molecules dissociates from this equilibrium configuration (in less than 1 ps) and forms a hydrogen bond to the second water molecule present.
- [44] M. Bühl, T. Steinke, P. v. R. Schleyer, R. Boese, *Angew. Chem.* **1991**, *103*, 1179; *Angew. Chem. Int. Ed. Engl.* **1991**, *30*, 1160.
- [45] J. C. Cruywagen, J. B. B. Heyns, A. N. Westra, *Inorg. Chem.* **1996**, *35*, 1556.
- [46] The classical propagation makes the conventional CPMD method not very well suited for the study of H transfer processes, for which quantum effects on the nuclei should be included explicitly (for instance, by path-integral methods; for a recent application see: D. Marx, M. E. Tuckerman, J. Hutter, M. Parrinello, *Nature* **1999**, *397*, 601). In any event, the occurrence of a deuterium transfer on the classical energy surface suggests that this is indeed a facile process.
- [47] V. Conte, F. Di Furia, S. Moro, *J. Mol. Catal. A* **1997**, *120*, 93.
- [48] a) (NH<sub>4</sub>)[VO(O<sub>2</sub>)<sub>2</sub>(NH<sub>3</sub>)]: R. E. Drew, F. W. B. Einstein, *Inorg. Chem.* **1972**, *11*, 1079; b) (ImH)[VO(O<sub>2</sub>)<sub>2</sub>Im] (Im = imidazole): D. C. Crans, A. D. Keramidis, H. Hoover-Litty, O. P. Anderson, A. M. Miller, L. M. Lemonine, S. Pleasic-Williams, M. Vandenberg, A. J. Rossomando, L. J. Sweet, *J. Am. Chem. Soc.* **1997**, *119*, 5447.
- [49] A. Butler, M. J. Clague, G. E. Meister, *Chem. Rev.* **1994**, *94*, 625.
- [50] V. Conte, F. Di Furia, S. Moro, *Inorg. Chim. Acta* **1998**, *272*, 62.
- [51] As in the case of **2**, sampling over more than 1 ps was necessary to converge the running average of **3** in H<sub>2</sub>O.

Received: February 26, 2001 [F3093]